

## Gridding Procedures for Non-Cartesian K-space Trajectories

Douglas C. Noll and Bradley P. Sutton

Dept. of Biomedical Engineering, University of Michigan, Ann Arbor, MI, USA

### 1. Introduction

The data collected during an MRI experiment is the spatial frequency information of the proton density of the object being imaged. The data space is referred to as k-space and is related to the image of the object through a Fourier transform relationship. When a Cartesian trajectory is used to traverse k-space, data are acquired on equally spaced grid points in k-space and a fast algorithm, the Fast Fourier Transform algorithm (FFT), can be used to reconstruct images from the data.

Non-Cartesian trajectories, such as spirals, radial lines (projection imaging), and rosettes may have benefits associated with flow artifact or efficiency of coverage of k-space, however, image reconstruction can no longer be accomplished with a simple FFT, which is applicable only to data on a Cartesian grid. We will discuss various issues in reconstructing data from non-Cartesian k-space trajectories, including a slow Fourier Transform, sample density considerations, methods that employ the FFT, and iterative reconstruction.

### 2. Reconstruction from non-Cartesian k-space

The signal equation in MRI that relates the proton density,  $m(\mathbf{r})$ , to the received signal,  $s(\mathbf{k})$ , is given by:

$$s(\mathbf{k}) = \int_{FOV} m(\mathbf{r}) e^{-i2\mathbf{p}\mathbf{k}\cdot\mathbf{r}} d\mathbf{r}, \quad [1]$$

where the integration occurs over the field-of-view (FOV) and  $\mathbf{k}(t) = \mathbf{g} \int_0^t \mathbf{G}(t) dt$ , where

$\mathbf{G}(t) = [G_x(t) \ G_y(t) \ G_z(t)]^T$  are the gradient waveforms. The reconstruction of this signal proceeds by an inverse Fourier Transform as:

$$\hat{m}(\mathbf{r}) = \int_{k\text{-space}} s(\mathbf{k}) e^{i2\mathbf{p}\mathbf{k}\cdot\mathbf{r}} d\mathbf{k}. \quad [2]$$

This continuous domain formula assumes that the area of integration  $d\mathbf{k}$  is uniform. Upon sampling at locations  $\mathbf{k}_j$  and discretizing the above expression, one needs to account for the possibility that samples have been acquired non-uniformly in k-space. This leads to the following reconstruction expression:

$$\hat{m}(\mathbf{r}) = \sum_j W(\mathbf{k}_j) s(\mathbf{k}_j) e^{i2\mathbf{p}\mathbf{k}_j\cdot\mathbf{r}} \quad [3]$$

This discretized reconstruction formula is a slow Discrete Fourier Transform and  $W(\mathbf{k}_j)$  is a weighting function that can account for non-uniform sampling. This reconstruction has also been referred to as the conjugate phase reconstruction (1) and the weighted correlation method (2). If data are acquired on the Cartesian grid, then this weighting function is a constant and Eqn. [3] can be evaluated using the FFT algorithm. For non-uniform sampling patterns, the FFT cannot be directly applied. Nevertheless, approximations exist that allow us to take advantage of the computational speed of the FFT and we will discuss these in a later section. We will first discuss this density compensation function,  $W(\mathbf{k}_j)$ , as there is still much interest in efficient and accurate ways to calculate it for arbitrary trajectories.

## 2.1 Density Compensation

In non-uniformly sampled imaging methods,  $W(\mathbf{k}_j)$  decreases the influence of data when redundant information is acquired. In projection and spiral imaging, for example, there are an excess of samples taken near the origin in k-space as shown in Figure 1.  $W(\mathbf{k}_j)$  should be selected to exactly compensate for this excess. In this example, the samples are denoted by (•) and one possible expression for  $W(\mathbf{k}_j)$  is the area in the cell surrounding each sample. Figure 2 contains an one-dimensional example of non-uniformly sampled data along with a reconstruction according to Equation [3]. In this example, there is an excess of samples near the origin, which is compensated for by the function in Fig. 2(b) to produce an undistorted resultant image (Fig. 2(d)).

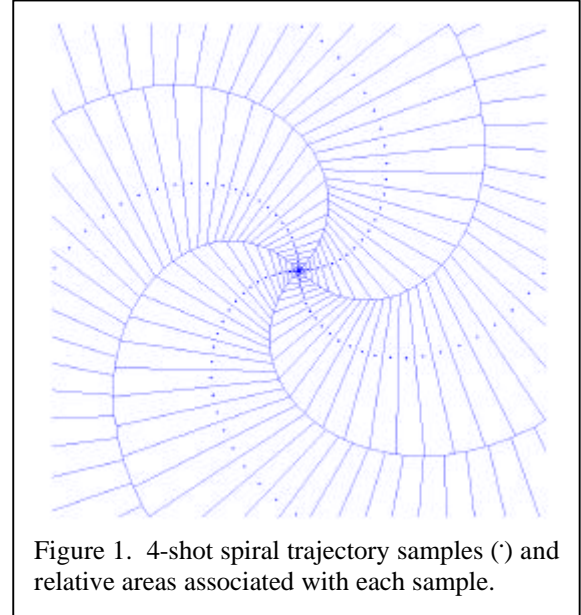


Figure 1. 4-shot spiral trajectory samples (•) and relative areas associated with each sample.

Many methods have been presented to address the determination of the sample density compensation functions (DCF) for arbitrary k-space trajectories. A straightforward and analytical method considers the formula of Eqn. [2] and uses a change of variables to go from the non-uniform variable  $\mathbf{k}$  to a uniform variable  $\mathbf{u}$ . The variable  $\mathbf{u}$  can represent a parameter of the

k-space trajectory that is varied uniformly, for example sample time and/or initial starting angle in the cases of a multi-shot spiral or radial line trajectory. This transformation leads to weighting function that is the Jacobian of this transformation

$$W(\mathbf{k}_j) = \left| \frac{\partial \mathbf{k}_j}{\partial \mathbf{u}} \right| \text{ as proposed}$$

by Norton (3) and Hoge et al. (4). This formula works well when the k-space trajectories can be described as simple functions of the uniformly sampled variables and when the trajectories do not cross. Many other methods have also been presented to quickly compute the DCF for arbitrary k-space trajectories.

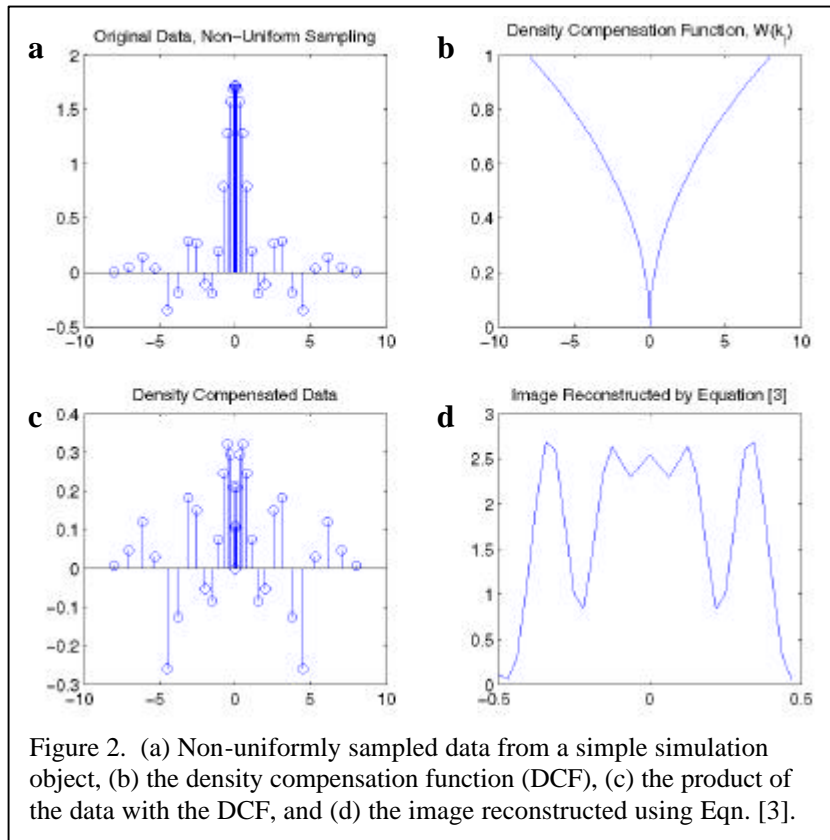


Figure 2. (a) Non-uniformly sampled data from a simple simulation object, (b) the density compensation function (DCF), (c) the product of the data with the DCF, and (d) the image reconstructed using Eqn. [3].

First, there is the familiar  $|\mathbf{r}|$  DCF for projection imaging. Jackson, et al. defined an area density function which was the convolution of delta functions at the k-space trajectory locations with the convolution function (5). Meyer, et al. developed an analytical expression for the DCF for Archimedean spiral trajectories (6). Rasche, et al. use areas of Voronoi cells around k-space sampling locations to determine the DCF for arbitrary k-space trajectories (7) (Figure 1 shows Voronoi cells for a spiral trajectory). Many other methods for computing the DCF exist (8-11).

### 3. The Gridding Reconstruction

The reconstruction of Eqn. [3] is generally desirable given appropriate DCF weights, however, this reconstruction is not computationally efficient. Nevertheless, we can benefit from computational advantage of the FFT when using non-Cartesian k-space trajectories if we first interpolate or “grid” the data onto a uniform grid and then apply the FFT. Despite low accuracy, simply using bilinear interpolation of the density-compensated data and then applying the FFT gives a reconstruction of the image. Other improved interpolation schemes have been used (12-14). A more commonly used and highly accurate method, called convolution gridding (5, 8, 15), is described by the following equation:

$$M_C = \{[(M \cdot S \cdot W) \otimes C] \cdot R\} \otimes^{-1} C \quad [4]$$

where  $M_C$  is the data gridded onto a Cartesian grid,  $M \cdot S$  is the sampled data on the k-space trajectory,  $W$  is the density compensation function,  $C$  is the convolution function, and  $R$  denotes the Cartesian grid sampling function. A gridding reconstruction involves 5 steps:

1. Multiply the sampled data with a density compensation function to account for the unequal sampling of k-space. This is usually the same DCF as that used in Eqn. [3].
2. Convolve the weighted data with a chosen convolution function.
3. Resample on a Cartesian (uniform) grid.
4. Apply the FFT.
5. Deapodization, to remove the effect of the convolution function by dividing the result by the Fourier Transform of the convolution function.

We first continue with our one-dimensional example. Figure 3 demonstrates, for the same 1D object, the first two steps of the gridding procedure. The result of

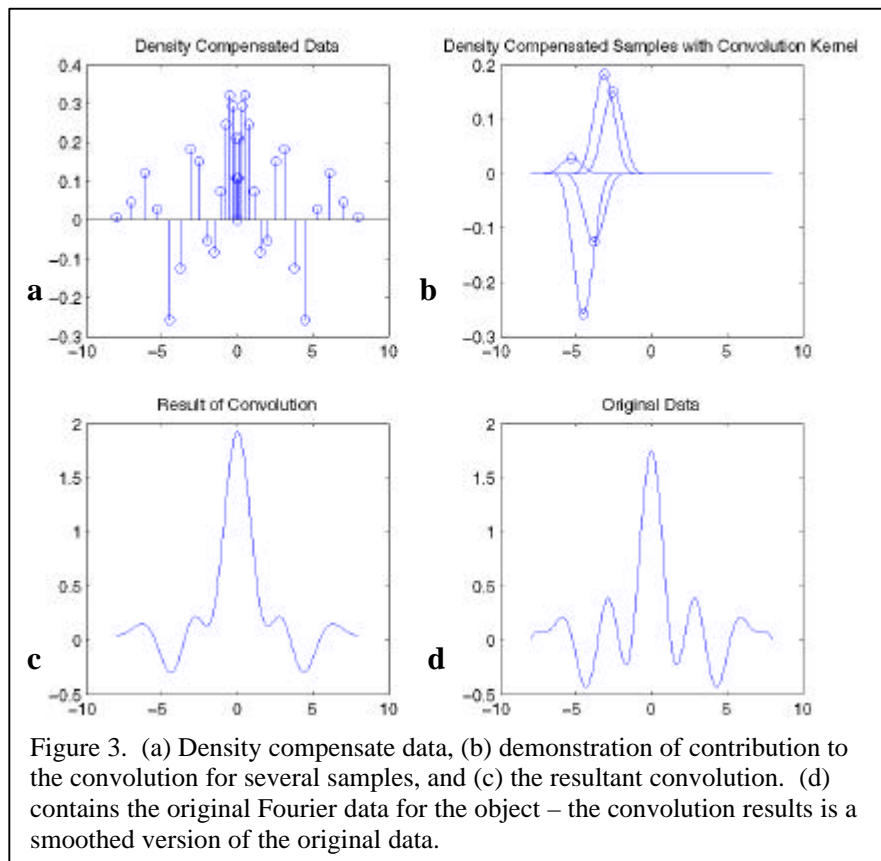
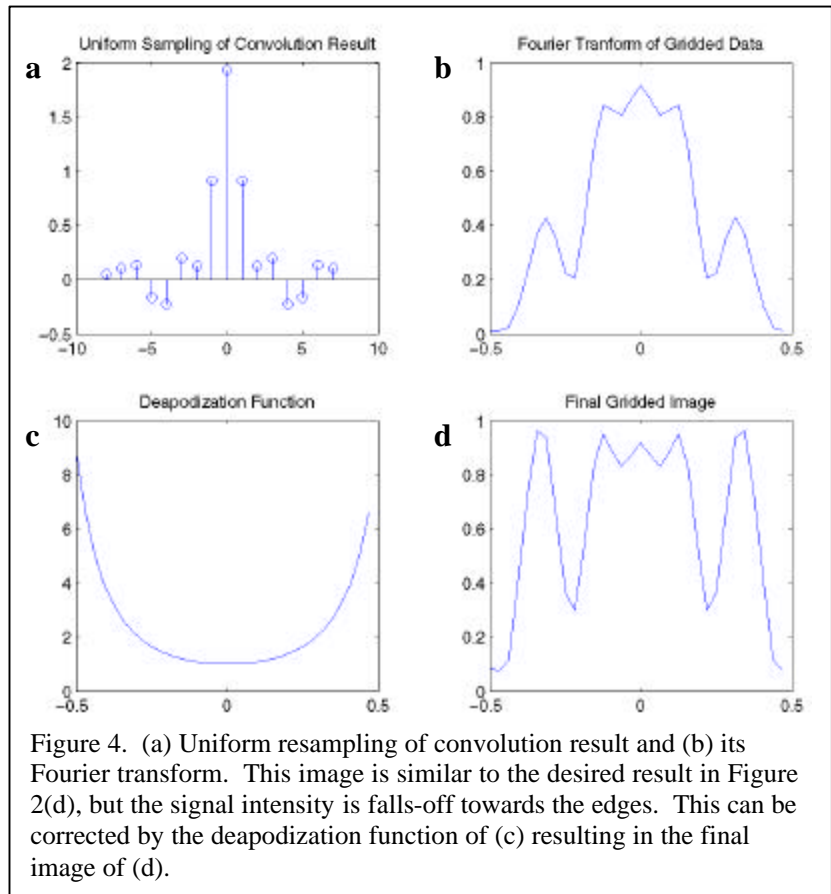


Figure 3. (a) Density compensate data, (b) demonstration of contribution to the convolution for several samples, and (c) the resultant convolution. (d) contains the original Fourier data for the object – the convolution results is a smoothed version of the original data.

the convolution is similar to the original Fourier data, it is smoothed by the convolution with a kernel shown in Fig. 3(b).

Figure 4 demonstrates the final three steps in the gridding procedure. The convolution result is re-sampled, but at uniform locations in k-space and the FFT is used to determine the image. The effect of convolution in the Fourier domain is the multiplication in the image domain. This leads to the fall-off in image intensity towards the edges of the image (apodization). In order to remove this effect, we divide by the Fourier Transform of the convolution function; this is known as deapodization. As one can see that this image (Fig. 4(d)) is very similar to the desired image of Fig. 2(d). With appropriate selection of the convolution function along with oversampling (discussed below), this final image can be made arbitrarily close to the desired image.



### 3.2 Practical Issues: Convolution Functions, Sampling and Oversampling

Here we discuss some of the practical issues related to implementation of gridding. First, while we describe the convolution and Cartesian resampling processes two as separate steps, these are usually implemented as one. Specifically, one only determines the value of the convolution at the Cartesian grid locations. Typically, this is implemented as an input data driven process – for each sampled data point, the nearby Cartesian grid locations are determined and the sample value times the convolution kernel value are added to each point.

When choosing a convolution function, one must consider the behavior of its Fourier transform both within the FOV and outside the FOV. The first issue is that the Fourier transform should have no zeros within the FOV, since division by the zero will result in large artifact. The second major issue relates to aliased energy. According to Fourier theory, sampling in k-space results in replication of the object in the image domain. By convolving the k-space samples with a convolution function, the resulting image replicates are multiplied by the Fourier transform (FT) of the convolution function. If the FT of the convolution function has significant energy that exists outside the FOV, then this energy will be aliased back into the image from the replicates.

During the deapodization process, the image is divided by the FT of the convolution function. Thus, optimization of the convolution kernel must consider the amount of energy outside the FOV and how much it is amplified by deapodization. Again, this aliased energy leads to image artifact and should be minimized. There are two approaches to address this problem: 1) using an oversampled Cartesian grid and 2) optimal selection of the convolution kernel parameters. The former, as presented by Jackson, et al. (5), is to grid the data onto a smaller grid. For example, if the grid size is reduced by a factor of 2, then the resulting FOV of the image is doubled. Energy that lies in the extension of the FOV is discarded and will not alias onto the image. This not only

reduces aliasing energy outright, but also allows a wider frequency response of the convolution function. Thus, the FT of the convolution function is more uniform over the desired FOV, with less amplification of aliased energy. Figure 5 demonstrates the effect of oversampling and the accuracy the gridding reconstruction. Fig. 5(b) shows energy that would be aliased into the image and amplified by the deapodization process without the oversampling. Jackson, et al. also examine various convolution functions with respect to minimizing aliased energy. They found that the Kaiser-Bessel kernel was simple to compute and worked very well. The optimal parameters for various sizes of the interpolation kernel are given in (5). In general, a higher accuracy is achieved using a larger kernel and larger oversampling factor, but it is at the expense of a higher computational burden – more samples involved in the interpolation and a larger FFT, respectively.

### 3.3 Computational Efficiency

Once the data has been resampled onto a Cartesian grid, we can take advantage of the computational efficiency of the FFT. Table 1 contains the operation counts for several reconstruction methods. This table shows that for a hypothetical example with 16,384 k-space samples and a 128x128 image, the gridding reconstruction reduces computation by nearly 3 orders of magnitude. In this example, we also compare the computational burden for gridding reconstruction to that of Cartesian sampled data. We see that for the gridding parameters selected the computational burden is roughly 6 times that of Cartesian sampled data. More

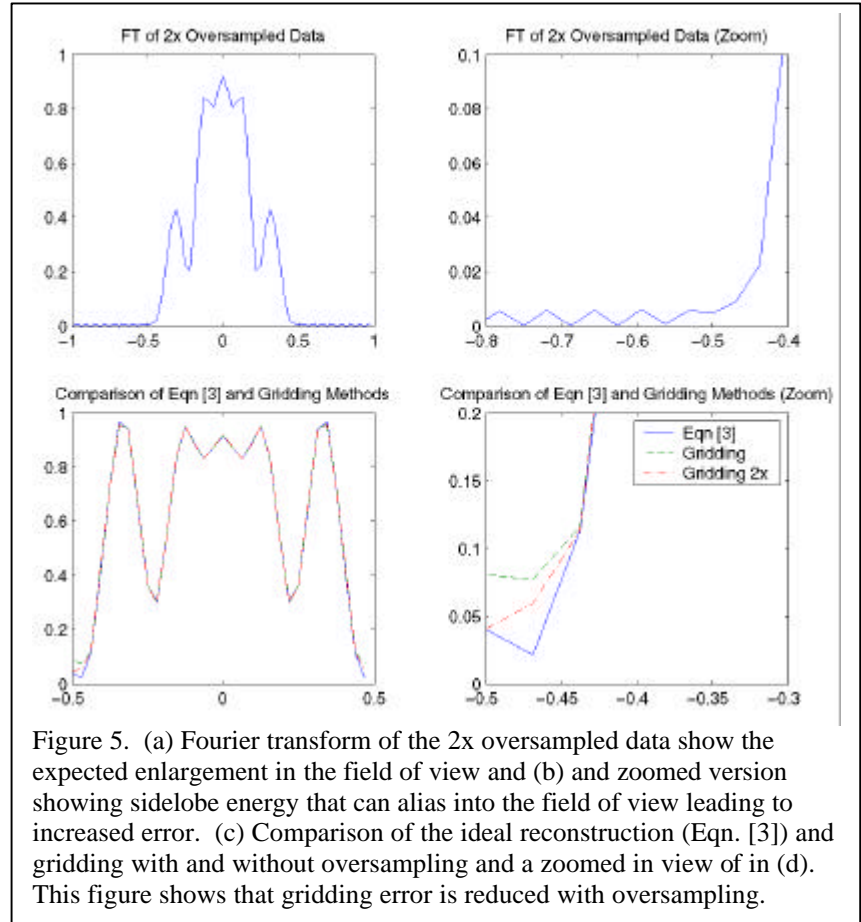


Figure 5. (a) Fourier transform of the 2x oversampled data show the expected enlargement in the field of view and (b) and zoomed version showing sidelobe energy that can alias into the field of view leading to increased error. (c) Comparison of the ideal reconstruction (Eqn. [3]) and gridding with and without oversampling and a zoomed in view of in (d). This figure shows that gridding error is reduced with oversampling.

aggressive gridding parameters, for example an oversampling factor of  $V = 1.5$ , can reduce the additional computational burden to roughly a factor of 4. With modern computational equipment, it is not particularly difficult to achieve real-time imaging with non-Cartesian k-space trajectories. Another practical issue associated with gridding and reconstruction by Eqn [3] is that there are many unique coefficients to be calculated (complex exponentials in Eqn. [3] and convolution grid locations and coefficients in gridding). This represents an additional computational burden, but as described in (16), this can be reduced by precalculation of necessary parameters and using look-up tables as these parameters are always fixed for a given trajectory.

Table 1. Operation counts for different reconstruction methods.

Method	Operations*	Operations- Example ( $M=16,384; N=128; W=3; V=2$ )
Equation [3]	$MN^2$	$2.7 \times 10^8$
Gridding with oversampling	$MW^2 + (VN)^2 \log_2(VN)$	$7.6 \times 10^5$
Cartesian sampling	$N^2 \log_2 N$	$1.1 \times 10^5$

\*M = total number of samples,  $N \times N$  = image matrix size, W = convolution kernel width, V = oversampling factor

#### 4. Other approaches

Other approaches to reconstructing data from arbitrary trajectories exist. We briefly describe two of these here, Uniform ReSampling (URS) (17) and iterative reconstruction (18, 19).

##### 4.1 URS/ BURS

URS proceeds by formulating the gridding interpolation problem as  $\mathbf{Ax}=\mathbf{b}$ , where  $\mathbf{x}$  is the value of the k-space data on a regular grid,  $\mathbf{b}$  is the data on the arbitrary trajectory (spiral, etc.), and  $\mathbf{A}$  is a matrix of interpolation coefficients, ie. *sinc* interpolation coefficients. Given the interpolation matrix and data at the arbitrary k-space locations, the inverse problem is solved by computing the pseudoinverse of  $\mathbf{A}$ . Once the regularly spaced data,  $\mathbf{x}$ , is determined, the image is formed by taking the FFT. No density compensation of the data or deapodization of the resulting image is necessary in this case. A variant of this algorithm called Block URS, or BURS, makes the solution more computationally feasible by limiting the size of  $\mathbf{A}$  by a local application of URS around each sample point.

##### 4.2 Iterative Reconstruction

Iterative image reconstruction uses the signal equation for MRI found in Eqn. [1] to find the image that best fits the data in the least-squares sense. An iterative method such as the conjugate gradient method (CGM) is used to minimize the following cost function:

$$\Psi(\mathbf{f}) = \frac{1}{2} \|\mathbf{y} - \mathbf{A}\mathbf{f}\|^2 + \mathbf{b} R(\mathbf{f}) \quad [5]$$

where  $\mathbf{A}$  is the system matrix with entries given in the simplest form by  $\mathbf{A}_{l,m} = \exp(-i 2\pi \mathbf{k}(t_l) \cdot \mathbf{r}_m)$ ,  $\mathbf{f}$  is the current estimate of the image, and  $R$  is a regularization function which penalizes roughness in the estimated image. No sample density function or deapodization is necessary with iterative reconstruction methods. Image reconstruction may take several to tens of iterations, but methods have been presented to speed computation of each iteration taking advantage of the FFT (20).



## 5. Conclusions

When nonuniform k-space trajectories such as spirals or radial lines are used in an MRI experiment, efficient image reconstruction is possible by gridding or interpolating the data onto a uniform grid and using the FFT. The gridding algorithm as optimized in (5) exhibits excellent accuracy, but also depends on the choice of a sample density compensation function (DCF). Fortunately, many methods exist for quickly computing the sample density function for arbitrary trajectories. Two other methods discussed, uniform resampling (URS) and iterative image reconstruction, do not use a sample density compensation function. The common method to reconstruct data from a non-Cartesian trajectory is to use the gridding method described in (5) with an oversampling factor of 1.5 or 2 and a Kaiser-Bessel convolution function.

## 6. References

1. Macovski A. Volumetric NMR imaging with time-varying gradients. *Magn Reson Med* 1983; 2:29-40.
2. Maeda A, Sano K, Yokoyama T. Reconstruction by weighted correlation for MRI with time-varying gradients. *IEEE Trans of Med Imaging* 1985; 7:26-32.
3. Norton SJ. Fast magnetic resonance imaging with simultaneously oscillating and rotating field gradients. *IEEE Trans Med Imaging* 1987; 6(1):21-31.
4. Hoge RD, Kwan RK, Pike GB. Density compensation functions for spiral MRI. *Magn Reson Med* 1997; 38(1):117-128.
5. Jackson J, Meyer C, Nishimura D, Macovski A. Selection of a convolution function for Fourier inversion using gridding. *IEEE Trans Med Imaging* 1991; MI-10(3):473-478.
6. Meyer C, Hu B, Nishimura D, Macovski A. Fast Spiral Coronary Artery Imaging. *Magn Reson Med* 1992; 28:202-213.
7. Rasche V, Proksa R, Sinkus R, Bornert P, Eggers H. Resampling of data between arbitrary grids using convolution interpolation. *IEEE Trans Med Imaging* 1999; 18(5):385-392.
8. Pipe JG, Menon P. Sampling density compensation in MRI: Rationale and an iterative numerical solution. *Mag Reson Med* 1999; 41:179--186.
9. Sedarat H, Nishimura DG. On the optimality of the gridding reconstruction algorithm. *IEEE Tr Med Im* 2000; 19(4):306-317.
10. Qian Y, Lin J, Jin D. Reconstruction of MR images from data acquired on an arbitrary k-space trajectory using the same-image weight. *Magn Reson Med* 2002; 48(2):306-311.
11. Schomberg H. Notes on direct and gridding-based Fourier inversion methods. in 2002 IEEE International Symposium on Biomedical Imaging. 2002. Washington, DC. p. 645-648.
12. Stark H, Woods JW, Paul I, Hingorani R. An investigation of computerized tomography by direct Fourier inversion and optimum interpolation. *IEEE Trans Biomed Engin* 1981; 28(7):496-505.
13. Stark H, Woods J, Paul I, Hingorani R. Direct Fourier reconstruction in computer tomography. *IEEE Trans Acoust Speech Sig Proc* 1981; 29:237-245.
14. Pan SX, Kak AC. A computational study of reconstruction algorithms for diffraction tomography - interpolation versus filtered backpropagation. *IEEE Trans Acoust Speech Sig Proc* 1983; 31:1262-1275.
15. O'Sullivan J. A fast sinc function gridding algorithm for Fourier inversion in computer tomography. *IEEE Trans Med Imaging* 1985; 4(4):200-207.
16. Dale B, Wendt M, Duerk JL. A rapid look-up table method for reconstructing MR images from arbitrary K-space trajectories. *IEEE Trans Med Imaging* 2001; 20(3):207-217.
17. Rosenfeld D. An optimal and efficient new gridding algorithm using singular value decomposition. *Magn Reson Med* 1998; 40(1):14-23.
18. Harshbarger TB, Twieg DB. Iterative reconstruction of single-shot spiral MRI with off resonance. *IEEE Trans Med Imaging* 1999; 18(3):196--205.
19. Sutton BP, Noll DC, Fessler JA. Fast, iterative field-correct image reconstruction for MRI. in IEEE Int. Symposium on Biomedical Imaging. 2002. Washington, DC. p. 489-492.
20. Fessler JA, Sutton BP. Nonuniform fast Fourier transforms using min-max interpolation (in press). *IEEE Trans Signal Proc* 2003.